Supplementary Information

Insights into the Synergistic Role of Metal-Lattice Oxygen Site Pairs in Four-Centered C-H Bond Activation of Methane: The Case of CuO

Jithin John Varghese,[1] Quang Thang Trinh,[1] and Samir H. Mushrif*
School of Chemical and Biomedical Engineering, Nanyang Technological University, 62 Nanyang Drive, 637459 Singapore
*Email: shmushrif@ntu.edu.sg

This file contains additional information regarding the computational methods, additional results supporting the discussion in the article with brief discussion, methods of calculation/analysis and references

Supplementary data includes

Supplementary information Figures S1 to S7

Supplementary information Tables S1 to S6

1. COMPUTATIONAL DETAILS

Copper has the fcc crystal structure and the bulk lattice constant of copper was optimized to 3.63 Å and was used for all subsequent calculations. Cu(111) surface was modelled as a periodic slab with 3 atomic layers in a 3x3 unit cell with a vacuum of 10 Å above the layers as shown in Fig.S1a. The first two layers were allowed to relax while the bottom most layer was fixed. A Monkhorst-Pack[1] type 4x4x1 special k-point grid was used for the sampling of Brillouin zone. Dissociatively chemisorbed oxygen on Cu(111) surface was modelled as one oxygen bound to fcc hollow site of Cu(111) surface in a 3x3 unit cell with three layers, as shown in Fig.S1b.

CuO has a monoclinic crystal structure and the bulk lattice constant was optimized at a = 4.68 Å, b = 3.43 Å, c = 5.14 Å, β = 99.3°, consistent with experimentally determined values.[2] The most stable and most frequently observed surfaces of CuO(111),[3,4] CuO($\bar{1}11$)[4] and CuO(110)[5] were chosen for detailed and comprehensive investigations. CuO(01$\bar{1}$) and CuO(010) surfaces are also experimentally observed and could be more reactive[6,7] than the most stable surfaces[8] and thus were also investigated for dissociation of methane. CuO(111), CuO($\bar{1}11$) and CuO(110) were

[1] Both the authors contributed equally to this work.

modelled as a periodic slabs with 3 atomic layers in a 3x2 unit cell with 12 Å of vacuum above it as shown in Fig.S1c-e.

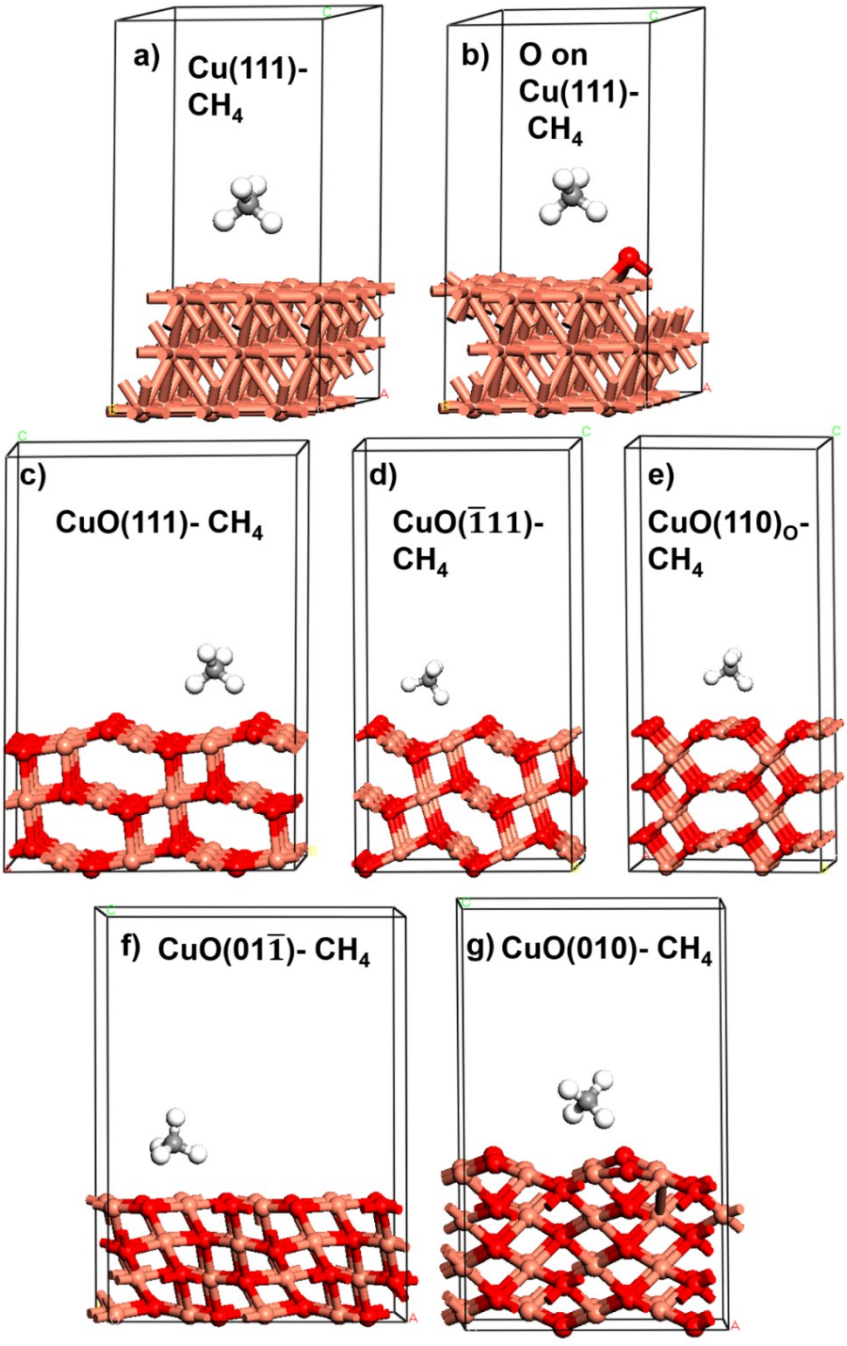

Fig. S1 Simulation supercells corresponding to **a)** Cu(111)- methane **b)** Chemisorbed oxygen on Cu(111)- methane **c)** CuO(111)- methane **d)** CuO($\bar{1}11$)- methane **e)** $CuO(110)_O$- methane **f)** CuO(01$\bar{1}$)- methane and **g)** CuO(010). The colour scheme is the same as that in Figure 3 of the article.

Two layers on the top were allowed to relax while the bottom layer was fixed. CuO($01\bar{1}$) and CuO(010) surfaces were modelled with four atomic layers in 3x2 units with 12 Å of vacuum above it as shown in Fig.S1f and g. The Brillouin zone was sampled with a 3x3x1 Monkhorst-Pack grid. The lowest layer was fixed and all other layers were allowed to relax in the simulations. All investigations of activation, first and subsequent dissociation reactions of methane were performed on these surfaces. All investigation of hydrogen abstraction of methane by only the chemisorbed/lattice oxygen on Cu(111) and CuO surfaces was performed with an initial configuration of methane with one of its C-H bond pointing directly to the oxygen species. The subsequent dissociation of CH_3 and CH_2 were investigated with a single CH_3 and CH_2 group on the under-coordinated copper atom/bridge of copper atoms respectively, without any co-adsorbed species on the surface. The coupling of CH_3 and CH_2 fragments on the CuO(111) surface was investigated in a 5x1 unit cell with three atomic layers and 10 Å of vacuum above it. The longer dimension in one of the coordinates corresponded to having larger number of under-coordinated Cu-O pairs and was chosen to avoid spurious effects due to lattice reconstruction (primarily Cu-Cu reconstruction) in this direction along the reaction coordinate. The Brillouin zone was sampled with a 1x3x1 Monkhorst-Pack grid.

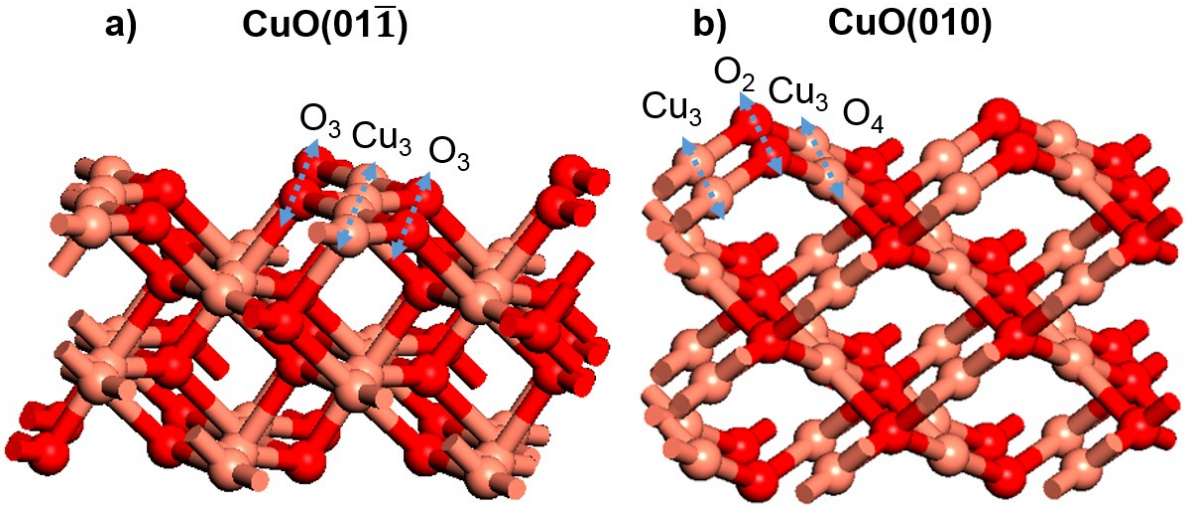

Fig. S2 Surface atomic arrangement and surface sites on CuO facets **a)** CuO($01\bar{1}$) surface with repeating arrangement of O_3-Cu_3-O_3. **b)** CuO(010) surface with repeating arrangement of Cu_3-O_2-Cu_3-O_4.

CuO($01\bar{1}$) surface exposes only 3-coordinated copper and oxygen atoms as shown in Fig. S2.a, while, CuO(010) surface shows a repeating arrangement of Cu_3-O_2-Cu_3-O_4 as shown in supplementary information Fig. S2b. Due to the presence of the under-coordinated pair of Cu-O atoms, the mechanism of methane activation on these facets is expected to the same as that on the most stable facets of CuO: CuO(111) and CuO($\bar{1}11$). However the activity of CuO($01\bar{1}$) and CuO(010) may differ from the stable surfaces on account of the greater coverage of low coordinated sites and due to the presence of the 2-coordinated oxygen atoms.

The energy of $CH_{4(gas)}$, $H_{2(gas)}$ and $H_2O_{(gas)}$ and $O_{2(g)}$ were calculated using a cubic box of 15 Å side and energy cut off of 450 eV. These were used to calculate the physisorption energy of CH_4 on the different surfaces, the chemisorption energy of CH_3 and H on the different surfaces, the binding energy of oxygen on the oxygen containing surfaces.

2. RESULTS AND DISCUSSION

2.1. Physisorption and activation of methane on the copper and copper oxide surfaces

The physisorption energy of methane on the Cu(111), chemisorbed oxygen containing Cu(111) and the three CuO surfaces were estimated based on the reaction scheme as below and is reported in Table S1.

$$CH_{4\ (g)} + \text{clean}_{\ m} \rightarrow CH_4\text{-}_m$$

Where $CH_{4\ (g)}$ represents an isolated methane molecule in the gas phase, $\text{clean}_{\ m}$ represents the clean surfaces under consideration: Cu(111), chemisorbed oxygen containing Cu(111), CuO(111), CuO($\bar{1}11$) and $CuO(110)_O$ surfaces without methane and CH_4-$_m$ represents weakly physisorbed methane on these surfaces. The physisorption energy is calculated as

$$\mathbf{E}_{\text{CH4-}m} - (\mathbf{E}_{\text{CH4 (g)}} + \mathbf{E}_{\text{clean }m})$$

It is reported in Table S1. The smaller the value, the stronger is the adsorption. The weakly physisorbed methane on these surfaces is considered as the initial state (IS). The activation energy barrier for dissociation of methane on the different Cu and CuO surfaces were calculated with respect to the energy of the IS. For comparison, the activation energy barriers computed with respect to a reactant state corresponding to methane in the gas phase is reported in Table S1. The calculation was based on the reaction scheme

$CH_{4\ (g)}$ + clean $_m$ → TS $_m$ → FS $_m$

TS $_m$ refers to the transition state corresponding to the dissociation where the dissociating CH_3 and hydrogen fragments of methane are bound to the surface, FS $_m$ refers to the final state with both the dissociated fragments, CH_3 and hydrogen are chemisorbed on the corresponding surface. The activation energy barriers is calculated as

$$\mathbf{E}_{\mathbf{TS}\,m} - (\mathbf{E}_{\mathrm{CH4\ (g)}} + \mathbf{E}_{\mathrm{clean}\,m})$$

The activation energy barriers calculated with both the reference systems are nearly the same and differ by less than 5 kJmol^{-1}. Thus all barriers reported in the article are with respect to the weakly physisorbed methane on the surfaces.

Table S1. Physisorption energy of methane on the clean Cu(111), chemisorbed oxygen containing Cu(111) and copper oxide surfaces. Comparison of activation energy barriers for dissociation of methane on the surfaces for a reference reactant state corresponding to weakly physisorbed methane on the surfaces with that of methane in the gas phase is also given.

Surface	**Physisorption energy of methane (kJ mol^{-1})**	**Activation energy barrier w.r.t. IS (kJ mol^{-1})**	**Activation energy barrier w.r.t. $CH_{4\ (g)}$ (kJ mol^{-1})**
Cu(111)	4.92	169.8	174.7
O on Cu(111)- 1 O on Cu(111)- 2	2.27 -0.14	133.1 144.9	135.6 144.7
CuO(111)- 1 CuO(111)- 2	2.21 0.96	76.6 130.9	79.2 132.4
CuO($\bar{1}11$)- 1 CuO($\bar{1}11$)- 2	-1.02 1.51	90.2 113.9	89.1 115.4
CuO(110)	2.36	109.1	111.5

2.2. Two-site four-centered C-H bond activation on CuO(01$\bar{1}$) and CuO(010) surfaces

In addition to CuO(111) and CuO($\bar{1}11$) surfaces, dissociation of methane was also investigated on other experimentally observed facets of CuO like CuO(01$\bar{1}$)[7] and CuO(010)[6] which are higher in surface energy[8] compared to CuO(111) and CuO($\bar{1}11$). The dissociation was observed

to proceed by involvement of the under-coordinated Cu-O pair as observed on CuO(111) and CuO($\bar{1}11$) surfaces. The structures corresponding to the IS, TS and FS for dissociation of methane on CuO(01$\bar{1}$) and CuO(010) are shown in Fig. S3a and S3b respectively. The activation energy barrier for dissociation of methane on CuO(01$\bar{1}$) was calculated to be 95.3 kJ mol^{-1} and that on CuO(010)) was calculated to be 60.3 kJ mol^{-1}. Although the dissociation barrier on CuO(01$\bar{1}$) is slightly higher than that on CuO(111) surface, the greater coverage of low-coordinated Cu-O pairs on the surface (Fig. S2a) may project CuO(01$\bar{1}$) to be a better catalyst for methane consumption. CuO(010) surface is observed to be the most active facet among the ones investigated here and this can be attributed to the involvement of the 2-coordinated oxygen on the surface (Fig. S2b). The reaction energy on CuO(01$\bar{1}$) surface was calculated to be ~3 kJ mol^{-1} while on CuO(010) surface is highly negative with the value -58.4 kJ mol^{-1}. The involvement of both copper and lattice oxygen in chemisorbing the fragments of dissociation lowers the reaction energy, making it more favourable.

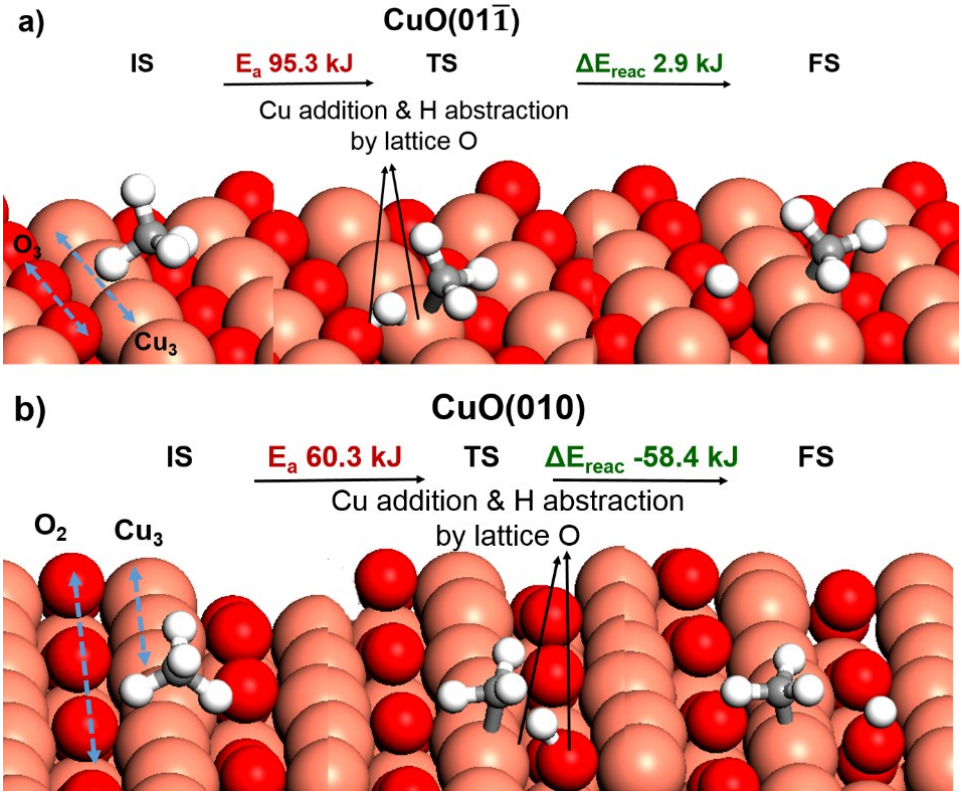

Fig.S3 Representation of the initial state (IS), transition state (TS) and final state (FS) corresponding to dissociative chemisorption of methane in a pathway involving synergistic roles

of **a)** the 3-coordinated copper (Cu_3) and lattice oxygen (O_3) atoms on CuO($01\bar{1}$) surface **b)** the 3-coordinated copper (Cu_3) and 2-coordinated lattice oxygen (O_2) atoms on CuO(010) surface. The activation barriers for dissociation of methane are also indicated in each case. Colour scheme is the same as that in Fig.3 of the manuscript.

2.3. Dissociation of methane in a pathway involving only chemisorbed oxygen on Cu(111)/lattice oxygen on CuO surfaces

Dissociation of methane on CuO($01\bar{1}$) and CuO(010) surface may also proceed by involvement of only the lattice oxygen. Lattice oxygen on these surfaces abstract hydrogen of methane with no assistance from the copper atoms, producing methyl radicals. The structures corresponding to the IS and TS for dissociation via this mechanism on CuO($01\bar{1}$) and CuO(010) surfaces is shown in Fig. S4a and b respectively. The barrier for dissociation of methane on CuO($01\bar{1}$) is 130.9 kJ mol^{-1} and is similar to that on CuO(111) surface. The barrier for dissociation on CuO(010) surface is much lower at 71.5 kJ mol^{-1}. The significantly low barrier here can be attributed to the involvement of the 2-coordinated lattice oxygen which is expected to be more active than the 3-coordinated oxygen.

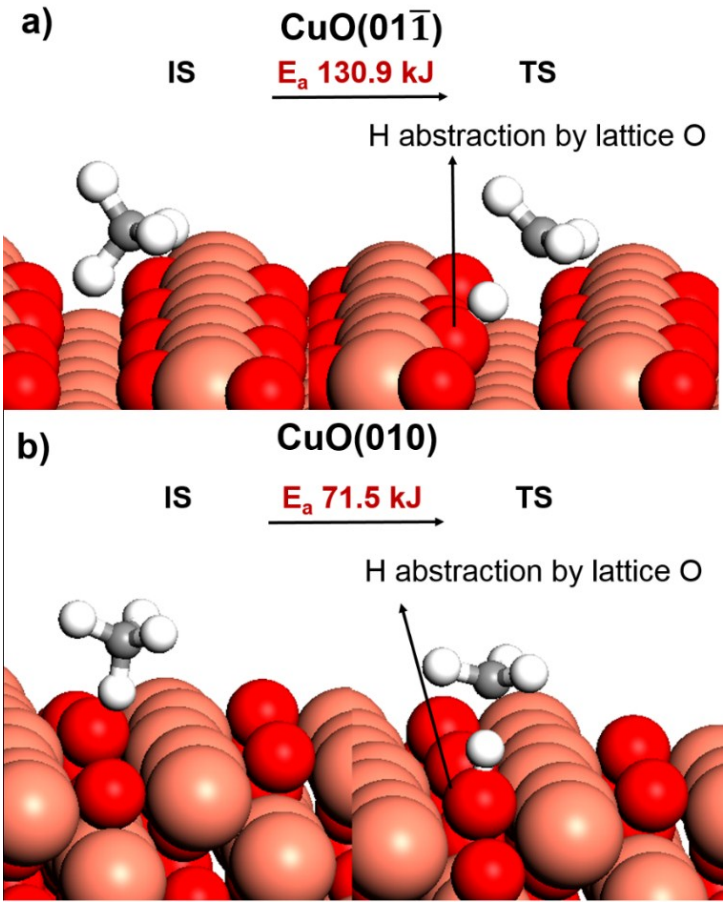

Fig.S4 Representation of the initial state (IS) and transition state (TS) corresponding to dissociation of methane in a pathway involving only hydrogen abstract by **a)** the 3-coordinated lattice oxygen (O_3) atoms on CuO(01$\bar{1}$) surface **b)** 2-coordinated lattice oxygen (O_2) atoms on CuO(010) surface. Colour scheme is the same as that in Fig.3 of the manuscript.

Dissociation of methane by only abstraction of hydrogen by the chemisorbed surface oxygen or the under-coordinated lattice oxygen atom on CuO surfaces leads to formation of a gas phase methyl species as shown in Fig. S5a, c, e and g. This methyl radical may subsequently chemisorb on the surface in configurations shown in Fig. S2b, d, f, and h. The chemisorption is highly favourable on the CuO surfaces as can be seen from the large negative energy change along the process.

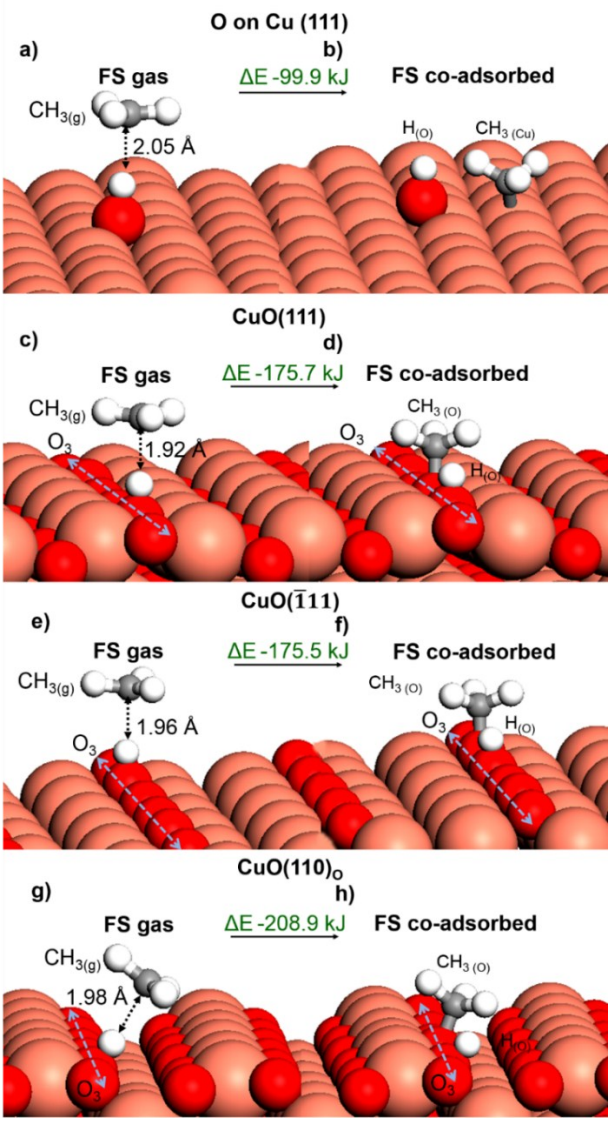

Fig. S5 Dissociation of methane via hydrogen abstraction mechanism alone, leading to formation of CH_3 radical on **a)** chemisorbed oxygen containing Cu(111) **c)** CuO(111) **e)** CuO($\bar{1}11$) and **g)** $CuO(110)_O$. The distance of carbon atom from the chemisorbed hydrogen is indicated in each case. The configuration corresponding to co-adsorption of the CH_3 radical on **b)** the copper atom on chemisorbed oxygen containing Cu(111) **d)** the under-coordinated lattice oxygen atom on Cu(111) **f)** the under-coordinated lattice oxygen atom on CuO($\bar{1}11$) and **h)** the under-coordinated lattice oxygen atom on $CuO(110)_O$. The difference in energy between the co-adsorbed configuration and the gas phase methyl radical is also indicated in each transformation.

2.4. Bader charges on CH_3 and hydrogen of methane and copper and oxygen atoms of clean and chemisorbed oxygen containing Cu(111), CuO($\bar{1}11$)and $CuO(110)_O$ in the different reaction pathways

Bader charges[9, 10] on the reaction centres (CH_3, H, Cu and O) as depicted in Fig.6 of the article, for the three different reaction mechanisms on clean and chemisorbed oxygen containing Cu(111), and the three CuO surfaces were calculated. The charges were calculated for the optimized configurations corresponding to IS, TS and FS. For the mechanism involving only copper atoms and for the mechanism involving both copper and oxygen atoms, the charges are summarised in Table S2. For the mechanism involving only oxygen atoms, the charges are summarised in information Table S3. In this case, the FS for which the charges are reported corresponds to a configuration with CH_3 in the gas phase and hydrogen chemisorbed on the lattice oxygen as on O-H.

Table S2. Bader charges on the CH_3 group and hydrogen of methane and the relevant surface copper and oxygen atoms on clean Cu(111), chemisorbed oxygen containing Cu(111), CuO(111) and CuO($\bar{1}11$) surfaces in the configurations corresponding to initial state (IS), transition state (TS) and final state (FS) in pathways involving only copper and both copper and oxygen atoms for activation of methane. **#1** represents average of the nine surface copper atoms, **#2** : average of the three copper atoms connected to the chemisorbed oxygen, **#3** : average of the two nearest copper atoms to methane, **#4** : average of the six copper atoms (Cu_3) on the surface of CuO(111) and CuO($\bar{1}11$), **#5** : average of the six four-coordinate copper atoms on the surface, **#6** : average of three copper atoms attached to CH_3, **#7** : average of the three copper atoms attached to hydrogen. ***1** : average of the six under-coordinated lattice oxygen atoms (O_3) on the surface of CuO(111) and CuO($\bar{1}11$).

IS				
Surface	**CH_3 (*e*)**	**H atom pointing to surface (*e*)**	**Surface Cu (*e*)**	**Surface O (*e*)**
Cu(111)	-0.0455	0.0227	-0.011 **#1**	NA
Chemisorbed O on Cu(111)	-0.133	0.1188	0.2460 **#2** /0.0076 **#3**	-0.9344
CuO(111)	-0.0279	0.087	0.8622**#4**/1.0317**#5**	0.9474 *1
CuO($\bar{1}11$)	-0.0062	0.1091	0.7941**#4**/1.0466**#5**	-0.8857 *1
TS				
Surface	**CH_3 (*e*)**	**Dissociating H (*e*)**	**Surface Cu (*e*)**	**Surface O (*e*)**
Cu(111)	-0.2861	-0.0856	0.1657	N.A.
Chemisorbed O on Cu(111)	-0.3504	0.4168	0.2364	-1.0069
CuO(111)	-0.229	0.4001	0.883/1.0276**#5**	-0.9901

CuO($\bar{1}11$)	-0.2093	0.4163	0.8759/1.0302[#5]	-0.9512
FS				
Surface	**CH_3 (*e*)**	**Dissociated H (*e*)**	**Surface Cu (*e*)**	**Surface O (*e*)**
Cu(111)	-0.3096	-0.2683	0.1502 [#6]/ 0.0864 [#7]	NA
O on Cu(111)	-0.3085	0.5997	0.2138 [#2]/ 0.1336 [#5]	-1.1842
CuO(111)	-0.1384	0.5972	0.8859	-1.0921
CuO($\bar{1}11$)	-0.1048	0.6748	0.8707	-1.1341

Table S3. Bader charges on the CH_3 group and hydrogen of methane and the relevant surface copper and oxygen atoms on chemisorbed oxygen containing Cu(111), CuO(111), CuO($\bar{1}11$) and $CuO(110)_O$ surfaces, in the configurations corresponding to initial state (IS), transition state (TS) and final state (FS), in a pathway involving only the oxygen atoms for activation of methane. The FS has CH_3 in the gas phase and hydrogen chemisorbed on the surface lattice oxygen as O-H. [#1] represents average of the three copper atoms connected to the chemisorbed oxygen, [#2] : average of the six surface under-coordinated copper (Cu_3) atoms, [#3] : average of the six surface four-coordinated copper (Cu_4) atoms.

IS				
Surface	**CH_3 (*e*)**	**H pointing to the surface (*e*)**	**Surface Cu (*e*)**	**Surface O to which H points (*e*)**
O-Cu	-0.0671	0.0552	0.2441[#1]	-0.9336
CuO(111)	-0.0665	0.0546	0.8561[#2]/1.0349[#3]	-0.9565
CuO($\bar{1}11$)	-0.0127	0.0098	0.7908[#2]/1.0458[#3]	-0.8914
$CuO(110)_O$	-0.1227	0.117	1.0645[#3]	-0.8354
TS				
Surface	**$CH_{3(g)}$ (*e*)**	**Dissociating H (*e*)**	**Surface Cu (*e*)**	**Surface O_3 atom abstracting H (*e*)**
O-Cu	-0.1465	0.4357	0.2154	-1.0596
CuO(111)	-0.0466	0.4526	0.8395[#2]/1.0161[#3]	-1.0309
CuO($\bar{1}11$)	-0.0963	0.3451	0.7778[#2]/1.0362[#3]	-0.9426
$CuO(110)_O$	0.0023	0.4537	1.0591[#3]	-0.9388
FS gas				
Surface	**$CH_{3(g)}$ (*e*)**	**Dissociated H (*e*)**	**Surface Cu (*e*)**	**Surface O_3 atom abstracting H (*e*)**
O-Cu	0.0131	0.6178	0.1877	-1.2104
CuO(111)	0.0431	0.5657	0.8342[#2]/1.0135[#3]	-1.1304
CuO($\bar{1}11$)	0.0497	0.5701	0.7669[#2]/1.0272[#3]	-1.103
$CuO(110)_O$	0.0368	0.609	1.0579[#3]	-1.0786

2.5. Interaction energy of CH_3 and hydrogen resulting from dissociation of methane at the transition state (TS) on the different surfaces

The interaction energy of CH_3 and hydrogen fragments of methane at the TS, resulting from dissociation, is decomposed based on the scheme

$$E_{int=} E^{TS} - \left(E_{CH3}^{TS} + E_{H}^{TS} - E_{surf}^{TS}\right)$$

Where E_{int} is the interaction energy of CH_3 and hydrogen species in the TS, E^{TS} is the total energy of the TS, E_{CH3}^{TS} is the energy of the CH_3 species on the surface at the TS without the hydrogen, E_{H}^{TS} is the energy of the hydrogen on the surface at the TS without the CH_3 species and E_{surf}^{TS} is the energy of the surface at the TS without both CH_3 and H. This scheme is based on the decomposition prescribed by Z-P Liu and P. Hu for 'Late' TS.[11] All the energy values were obtained from single point calculations without optimization of geometry. The positive values suggest repulsive interaction and negative values suggest attractive interaction.

Table S4. Interaction energy of the dissociating CH_3 and hydrogen fragments of methane at the transition state (TS) on the clean and chemisorbed oxygen containing Cu(111), CuO(111) and CuO($\bar{1}11$).

Surface	Interaction energy of CH_3 with H (kJ mol^{-1})
Cu(111)	32.6
Chemisorbed O Cu	-123.8
CuO(111)	-101.1
CuO($\bar{1}11$)	-78.9

2.6. Geometry of methane at the initial state (IS) and transition state (TS) on the clean and chemisorbed oxygen containing Cu(111), CuO(111) and CuO($\bar{1}11$) surfaces

The geometric parameters of the methane molecule (the four C-H bond length and six H-C-H angles) at the IS and the TS are when it interacts and dissociates on clean Cu(111), chemisorbed

oxygen containing Cu(111), CuO(111) and CuO($\bar{1}11$) surfaces in pathways involving only the copper atom or both copper and oxygen atoms were calculated. The values are summarised in information Table S5. The equilibrium C-H bond length of methane from our calculation is 1.1 Å and the equilibrium H-C-H angles is 109.5°. The deformation of the molecule at the TS gives an estimate of the strain on the molecule. One of the C-H bonds of methane (highlighted in red) can be seen to stretch considerably at the TS before it dissociates. The amount of stretching reduces when oxygen is involved along with copper in activation. The deformation of the H-C-H angles (highlighted in blue) are nearly the same for all the oxygen containing surfaces.

Table S5. The dimensions of the four C-H bonds and six H-C-H angles of methane as observed in the initial state (IS) IS and the transition state (TS) on clean Cu(111), chemisorbed oxygen containing Cu(111), CuO(111) and CuO($\bar{1}11$) surfaces. CH n (n=1 to 4) refers to the C-H bonds of methane and HCH m (m=1-6) refers to the H-C-H angles of methane. The dissociating C-H bond length at the TS on each of the surfaces is highlighted in red and the H-C-H angles involving the dissociating C-H bond, suggesting deformation of methane, is highlighted in blue.

	IS									
Surface	**CH 1 (Å)**	**CH 2 (Å)**	**CH 3 (Å)**	**CH 4 (Å)**	**HCH 1 (°)**	**HCH 2 (°)**	**HCH 3 (°)**	**HCH 4 (°)**	**HCH 5 (°)**	**HCH 6 (°)**
Cu(111)	1.1	1.095	1.095	1.097	109.02	109.04	109.21	109.36	109.38	110.78
O on Cu(111)	1.095	1.094	1.096	1.102	110.49	108.81	109.18	109.13	110.28	108.89
CuO(111)	1.098	1.104	1.095	1.093	110.51	109.44	109.01	108.28	111.16	108.41
CuO($\bar{1}11$)	1.104	1.094	1.091	1.093	107.51	110.15	107.50	109.87	110.81	110.86
CuO(01$\bar{1}$)	1.096	1.096	1.097	1.1	109.34	109.77	110.12	108.19	109.31	110.08
CuO(010)	1.095	1.095	1.101	1.103	108.51	109.12	111.42	108.53	108.67	110.59
	TS									
Cu(111)	1.804	1.095	1.095	1.099	105.30	82.01	134.53	111.31	108.69	110.70
O on Cu(111)	1.41	1.098	1.101	1.104	99.95	94.37	138.74	110.32	106.27	105.34
CuO(111)	1.372	1.099	1.097	1.099	92.78	96.56	138.37	107.46	108.46	111.45
CuO($\bar{1}11$)	1.392	1.098	1.099	1.1	95.41	95.44	136.65	112.10	108.03	107.96
CuO(01$\bar{1}$)	1.427	1.099	1.099	1.1	94.419	98.922	136.17	106.92	107.39	111.93
CuO(010)	1.39	1.098	1.10	1.105	96.41	102.15	132.18	106.87	107.17	111.06

2.7. Nearly linear relationship of the activation energy barrier with the reaction energy and of the energy of the transition state with energy of the final state in methane activation on copper and copper oxide surfaces

Figure 7 in the manuscript shows the nearly linear relationship of the activation energy barrier for dissociation of methane with the reaction energy on the Cu(111), chemisorbed oxygen containing Cu(111), CuO(111) and CuO($\bar{1}11$) surfaces. A similar relationship is observed on CuO(01$\bar{1}$) and CuO(010) surfaces as well. The BEP like relationship observed on all the copper and copper oxide surfaces (except $CuO(110)_O$ is presented in Fig. S6. The TS on the CuO(01$\bar{1}$) and CuO(010) surfaces is also 'late', resembling the FS, with almost dissociated C-H bonds and nearly formed O-H species as can be seen from Fig. S2. Minor deviations from linearity may be attributed to the differences in geometrical arrangement of the Cu-O pairs on the different CuO surfaces. Such differences can bring about changes to the extent of stabilization of the transition state and the fragments of dissociation.

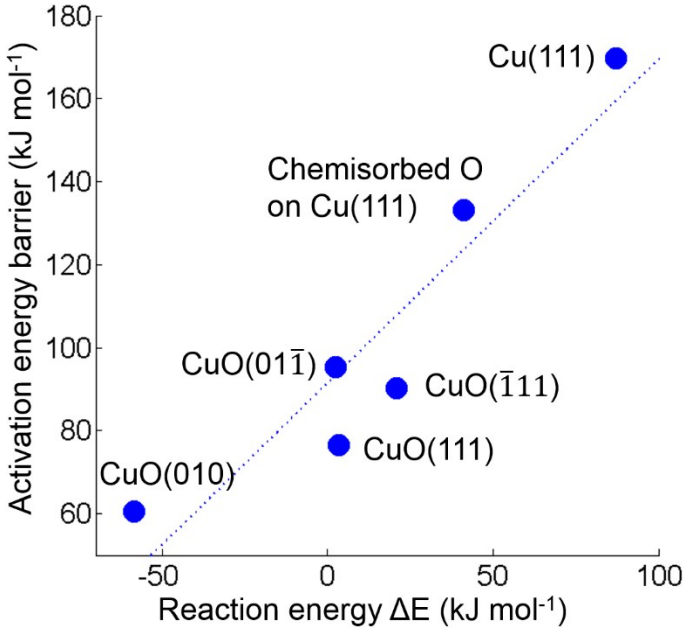

Fig. S6 Plot of the activation energy barrier for dissociation of methane on the various copper and copper oxide surfaces against the corresponding reaction energy. The plot shows a nearly linear correlation of the two quantities.

We also observed a linear relationship between the absolute energy of the structure corresponding to the TS with that of the structure corresponding to the FS on the copper and copper oxide surfaces. This suggest that the TS resembles the product and is thus 'late'. The plot of the relationship is presented in Fig.S7.

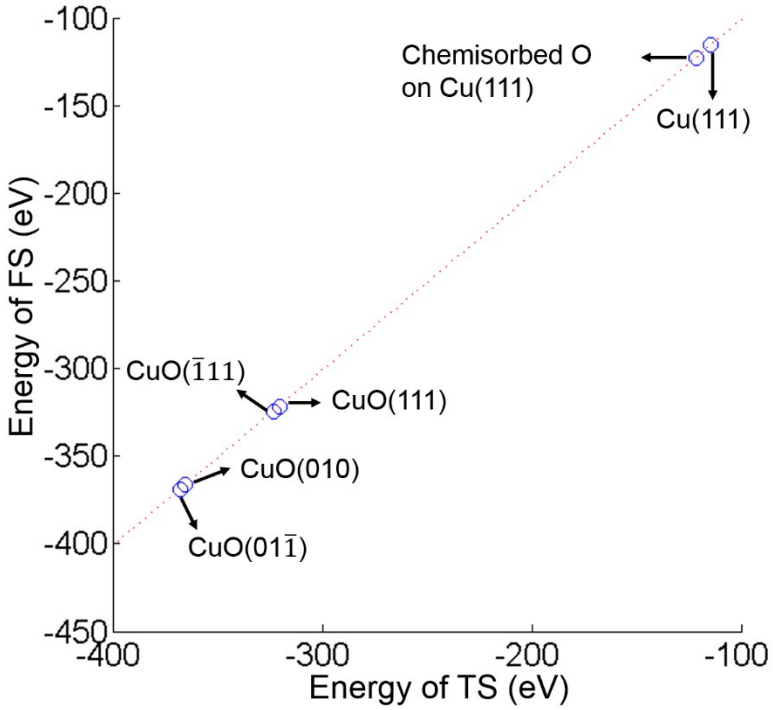

Fig. S7 Plot of the energy of the transition state (TS) against the energy of the corresponding final state (FS) in methane activation on clean Cu(111), in the pathway involving both copper and oxygen atoms on chemisorbed oxygen containing Cu(111), CuO(111) and CuO($\bar{1}11$), CuO($01\bar{1}$) and CuO(010) surfaces, showing a linear correlation of the two quantities.

The absolute energy of the TS corresponding to dissociation of methane on clean Cu(111), in the pathway involving both copper and oxygen atoms on chemisorbed oxygen containing Cu(111), CuO(111) and CuO($\bar{1}11$) surfaces is observed to have a nearly linear correlation with the absolute energy of the final product state. Fig.S2 shows this correlation. This suggests the TS is 'late' on these surfaces in this dissociation pathway.

2.8. Binding energy of chemisorbed/lattice oxygen on Cu(111), CuO(111), CuO($\bar{1}11$) and $CuO(110)_O$ surfaces and chemisorption energy of the dissociated CH_3 and hydrogen on these surfaces.

The binding energy of the chemisorbed/under-coordinated lattice oxygen on the surface of Cu(111) and different CuO facets was estimated based on the method suggested by J. K. Nørskov and co-workers[12] using the reaction scheme

$$Cu/Cu_nO_{n-1} + H_2O_{(g)} \rightarrow O\text{-}Cu/Cu_nO_n + H_{2(g)}$$

Where Cu/Cu_nO_{n-1} is the clean Cu(111) surface/CuO surface with one under-coordinated lattice oxygen vacancy, O-Cu is the chemisorbed oxygen containing Cu(111) surface, Cu_nO_n is the stoichiometric CuO facets and $H_{2(g)}$ and $H_2O_{(g)}$ are molecules in the gas phase. For the copper oxide surfaces, the reaction energies can also be interpreted as the energy for inserting oxygen into a vacancy on the surface or the energy for creating an oxygen vacancy. Either ways, the value is indicative of the strength of binding of the lattice oxygen on the surface by virtue of its interaction with the copper atoms. Absolute values of such interactions from DFT calculations may not be physically accurate/comparable or relevant and thus, such values are best used to qualitatively represent trends on the binding strength of oxygen and its consequences.[13]

An alternate method to calculate the binding energy of oxygen on the surface is based on the scheme suggested by F. Frechard and R.A. van Santen[14] with reference to the gas phase O_2 molecule as $E_{O\text{-}binding} = -[E_{O\text{-}Cu/CunOn} - (E_{Cu/CunOn-1} + E_{½\ O2(g)})]$. This would be equivalent to the reaction scheme

$Cu/Cu_nO_{n-1} + ½\ O_{2(g)} \rightarrow O\text{-}Cu/Cu_nO_n$

The same qualitative trend with similar relative differences in binding energy is obtained for the different surfaces by this method as well. The binding energy of oxygen on the CuO surfaces is found to follow the trend CuO(111) > CuO($\bar{1}11$) > $CuO(110)_O$. Binding energy data obtained by both the methods is presented in the Table S6.

Table S6. Comparison of the values of oxygen binding energy on the surface/energy for inserting oxygen into a vacancy on the oxide surface by two methodologies a) as per the equation $Cu/Cu_nO_{n-1} + H_2O_{(g)} \rightarrow O\text{-}Cu/Cu_nO_n + H_{2(g)}$ and b) as per the equation $Cu/Cu_nO_{n-1} + ½\ O_{2(g)} \rightarrow O\text{-}Cu/Cu_nO_n$

Surface	Oxygen binding energy/energy for creating oxygen vacancy from original methodology in the manuscript (kJ)	Relative difference (kJ)	Oxygen binding energy/energy for creating oxygen vacancy from referee suggested methodology (kJ)	Relative difference (kJ)
Chemisorbed O on Cu(111)	84.82		-158.73	
CuO(111)	26.60	$E_{CuO111} - E_{(CuO\text{-}111)} = -25.08$	-216.96	$E_{CuO111} - E_{(CuO\text{-}111)} = -25.09$
CuO($\bar{1}11$)	51.68	$E_{CuO111} - E_{(CuO\text{-}111)} = -95.4$	-191.87	$E_{CuO111} - E_{(CuO\text{-}111)} = -95.39$

$CuO(110)_O$	147.08	E_{CuO110} - E_{CuO111} = 120.48	-96.48	E_{CuO110} - E_{CuO111} = 120.48

.

Chemisorption energy of the dissociated hydrogen on the under-coordinated lattice oxygen (O_3) atom on the three CuO surfaces and on the dissociatively chemisorbed oxygen on Cu(111) surface was estimated using the reaction scheme

$$\frac{1}{2} H_{2(g)} + * \rightarrow H*$$

Where $H_{2(g)}$ is the energy of the H_2 molecule calculated in the gas phase, * refers to the energy of the clean surface (chemisorbed oxygen containing Cu(111), CuO(111), CuO($\bar{1}11$) and $CuO(110)_O$) and H* refers to the energy of one hydrogen chemisorbed on the oxygen (chemisorbed/ lattice) on these surfaces.

The chemisorption energy of CH_3 on the chemisorbed /under-coordinated lattice oxygen atom on the Cu(111) and CuO surfaces respectively was calculated based on the reaction scheme

$$CH_{4(g)} + * \rightarrow CH_3* + \frac{1}{2} H_{2(g)}$$

Where $CH_{4(g)}$ refers to the energy of CH_4 molecule in the gas phase, * refers to the clean surface, CH_3* refers to the CH_3 individually chemisorbed on the chemisorbed/ lattice oxygen on these surfaces and $H_{2(g)}$ refers to the hydrogen molecule in the gas phase.

Chemisorption energy of CH_3 on the copper/under-coordinated copper (Cu_3) atoms on the chemisorbed oxygen containing Cu(111) and CuO surfaces respectively was calculated as per the scheme

$$CH_{4(g)} + * \rightarrow CH_3* + \frac{1}{2} H_{2(g)}$$

Where $CH_{4(g)}$ refers to the energy of CH_4 molecule in the gas phase, * refers to the clean surface, CH_3* refers to the CH_3 individually chemisorbed on the copper/under-coordinated copper atom on these surfaces and $H_{2(g)}$ refers to the hydrogen molecule in the gas phase.

The data from all of these calculations is presented in Table 3 of the manuscript.

REFERENCES

1. H. J. Monkhorst and J. D. Pack, *Phys. Rev. B*, 1976, **13**, 5188-5192.
2. S. Åsbrink and L. J. Norrby, *Acta Crystallogr., Sect. B: Struct. Sci., Cryst. Eng. Mater.*, 1970, **26**, 8-15.
3. X. Jiang, T. Herricks and Y. Xia, *Nano Lett.*, 2002, **2**, 1333-1338.
4. P. N. Amaniampong, Q. T. Trinh, B. Wang, A. Borgna, Y. Yang and S. H. Mushrif, *Angew. Chem. Int. Ed.*, 2015, **54**, 8928-8933.
5. R. Bari, S. Patil and A. Bari, *Int. Nano Lett.*, 2013, **3**, 1-5.
6. Q. Zhang, K. Zhang, D. Xu, G. Yang, H. Huang, F. Nie, C. Liu and S. Yang, *Prog. Mater. Sci.*, 2014, **60**, 208-237.
7. K. Zhou, R. Wang, B. Xu and Y. Li, *Nanotechnology*, 2006, **17**, 3939-3943.
8. J. Hu, D. Li, J. G. Lu and R. Wu, *J. Phys. Chem. C*, 2010, **114**, 17120-17126.
9. R. F. W. Bader, *Atoms in Molecules: A Quantum Theory*, Oxford University Press, USA, 1990.
10. G. Henkelman, A. Arnaldsson and H. Jónsson, , *Comput. Mater. Sci.*, 2006, **36**, 354-360.
11. Z. P. Liu and P. Hu, *J. Am. Chem. Soc.*, 2003, **125**, 1958-1967.
12. J. K. Nørskov, J. Rossmeisl, A. Logadottir, L. Lindqvist, J. R. Kitchin, T. Bligaard and H. Jónsson, *J. Phys. Chem. B*, 2004, **108**, 17886-17892.
13. E. W. McFarland and H. Metiu, *Chem. Rev.*, 2013, **113**, 4391-4427.
14. F. Frechard and R. A. Van Santen, *Surf. Sci.*, 1998, **407**, 200-211.